The melting of ice in a hot humid stream of air

By DONALD L. TURCOTTE
U.S. Naval Postgraduate School, Monterey, California*

(Received 13 October 1959)

By use of appropriate approximations the incompressible stagnation-point ablation rate for ice is determined theoretically. The theory includes both melting and vaporization or condensation. To verify the theory hemispheres of ice were melted in a subsonic wind tunnel with controlled humidity. It is found that the effects of heat transfer and condensation are of equal importance in determining the melt rate. The agreement between theory and experiment is adequate.

1. Introduction

In order to understand the many mechanisms involved in ablation it seems appropriate to study some of the simpler problems in detail. It is the purpose of this paper to analyse the incompressible stagnation-point melting of ice from a hemisphere in hot, humid air. The convective heat transfer to the ice body will certainly melt it. However, vaporization or condensation of water can have an important effect on the melt rate. The problem considered here is illustrated in figure 1.

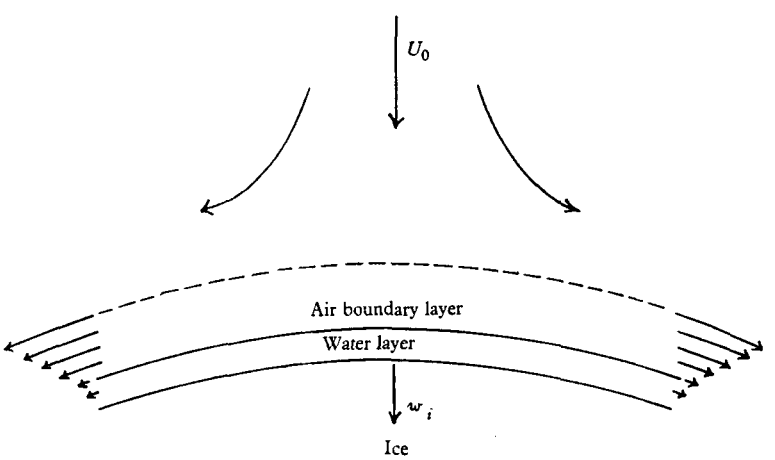

FIGURE 1. Illustration of stagnation-point ablation.

To obtain any solution to the problem many assumptions must be made. The work of Roberts (1958) provides an insight into what approximations are valid if mass transfer is neglected. In this paper these approximations are applied to the problem with diffusion effects included. The diffusion problem of mass transfer in boundary-layer flows has been discussed in detail by Lees (1958).

* Now at Cornell University, Ithaca, New York.

2. Theory

The solution of the incompressible boundary-layer equations for the stagnation region of a hemisphere is well known (Schlichting 1955, p. 162). The solution for a melting material which does not vaporize has been given by Roberts (1958). The results obtained by Roberts indicate what approximations may be valid in the present problem. A solution to the present problem will be obtained neglecting the presence of the water layer. This is equivalent to the following assumptions.

(i) The velocity at the air–water interface is small compared with the velocity at the outer edge of the air boundary layer.

(ii) The temperature increase across the water layer is small compared with the temperature increase in the air boundary layer.

(iii) The heat convected away in the water layer is small compared with the heat flux across the layer. Having obtained a solution utilizing this approximation, its validity will be checked.

With the presence of the water layer neglected, the boundary conditions at the water–ice interface may be applied at the air–water interface. Since it is assumed that the ice is at its melt temperature, the heat transfer $\dot{q}_W[l]$ on the liquid side of the air–water interface may be related directly to the melt rate w_i of the ice by the relation

$$\dot{q}_W[l] = \rho_i L_f w_i, \tag{1}$$

where L_f is the heat of fusion for water and ρ_i the density of ice.

The solution for the air boundary layer, including heat transfer and diffusion, may be obtained following the method of Lees (1958). For simplicity air will be denoted by the subscript A and water vapour by the subscript B. The enthalpy is then defined by $h = K_A h_A + K_B h_B$, where K_A and K_B are the concentrations by weight of air and water vapour ($K_A + K_B = 1$). Near the stagnation point of a hemisphere the appropriate boundary-layer equations for the conservation of mass, momentum, energy, and species concentration are

$$\frac{\partial(xu)}{\partial x} + \frac{\partial(xv)}{\partial y} = 0, \tag{2}$$

$$u\frac{\partial u}{\partial x} + v\frac{\partial u}{\partial y} = \frac{9}{4}\frac{U_0^2}{R^2}x + \nu\frac{\partial^2 u}{\partial y^2}, \tag{3}$$

$$u\frac{\partial h}{\partial x} + v\frac{\partial h}{\partial y} = \frac{\nu}{\sigma}\frac{\partial^2 h}{\partial y^2} + D_{AB}\left(1 - \frac{1}{\lambda}\right)\frac{\partial}{\partial y}\left[h_A\frac{\partial K_A}{\partial y} + h_B\frac{\partial K_B}{\partial y}\right], \tag{4}$$

$$u\frac{\partial K_B}{\partial x} + v\frac{\partial K_B}{\partial y} = \frac{\nu\lambda}{\sigma}\frac{\partial^2 K_B}{\partial y^2}, \tag{5}$$

where σ is the Prandtl number $\bar{C}_p\mu/\kappa$ and λ the Lewis number $\rho D_{AB}\bar{C}_p/\kappa$. For the diffusion of water vapour in air the binary diffusion coefficient D_{AB} has the value $0{\cdot}240 \times 10^{-3}$ ft.^{2}/sec. The corresponding value of the Lewis number is 1·20. In order to make the above set of equations amenable to analysis the remainder of the solution will be restricted to the case $\lambda = 1{\cdot}00$. The adequacy of this approximation may be deduced from comparison with experiment.

In order to reduce the above set of equations to their 'similarity' form the following set of dimensionless variables are introduced

$$\eta = \sqrt{\left(\frac{3}{2}\frac{U_0}{\nu R}\right)}\, y, \quad u = \frac{3}{2}\frac{U_0}{R} f'(\eta)\, x, \quad v = -2\sqrt{\left(\frac{3}{2}\frac{U_0 \nu}{R}\right)} f(\eta),$$

$$h = h_W - (h_W - h_0)\, g(\eta), \quad K_B = K_{BW} - (K_{BW} - K_{B0})\, n(\eta). \tag{6}$$

Assuming K_{BW} and h_W to be constant we may write equations (2–5) as a set of ordinary differential equations:

$$f'^2 - 2ff'' = 1 + f''', \tag{7}$$

$$g'' + 2\sigma f g' = 0, \tag{8}$$

$$n'' + 2\sigma f n' = 0. \tag{9}$$

The appropriate boundary conditions are:

$$\left.\begin{aligned} &\text{at} \quad \eta = 0, \quad f = f' = g = n = 0; \\ &\text{at} \quad \eta = \infty, \quad f' = g = n = 1. \end{aligned}\right\} \tag{10}$$

Actually vaporization corresponds to fluid injection so that $f(0) \neq 0$. But it will be assumed that $f(0) \ll 1$ so that the flow in the air boundary layer is unaffected. If this approximation is not adequate then an iteration procedure can be used to obtain a solution.

The numerical solution to (7) with the boundary conditions (10) is given by Schlichting (1955). The solutions to equations (8) and (9) have been obtained by Sibulkin (1952). The resultant values for the wall gradients of enthalpy and concentration are

$$\left.\frac{\partial h}{\partial y}\right|_W = 0{\cdot}812(h_0 - h_W)\sqrt{\frac{U_0}{R\nu}}, \tag{11}$$

$$\left.\frac{\partial K_B}{\partial y}\right|_W = 0{\cdot}812(K_{B0} - K_{BW})\sqrt{\frac{U_0}{R\nu}}, \tag{12}$$

where σ has been assumed to be 0·700. The differential of the enthalpy may be written $dh = \overline{C_p}\, dT + (h_A - h_B)\, dK_B$. Using this relation and the similarity between enthalpy and concentration gradients the temperature gradient at the wall may be written

$$\left.\frac{\partial T}{\partial y}\right|_W = 0{\cdot}812(T_0 - T_W)\sqrt{\frac{U_0}{R\nu}}. \tag{13}$$

To obtain the rate at which the ice melts, the gradients of temperature and concentration must be related to the rate at which heat is transferred through the water layer. A relation may be written for the conservation of water across the air–water interface. The balance of diffusion of water vapour against the normal current of water vapour above and water below the interface gives

$$(\rho v)_W = (\rho v)_W K_{BW} - \rho D_{AB} \left.\frac{\partial K_B}{\partial y}\right|_W. \tag{14}$$

This balance is illustrated in figure 2. In a similar manner the energy balance may be written. Equating the transport of heat by conduction and diffusion to the normal currents of energy in the air and water we obtain

$$\dot{q}_W[l] = \left[k\frac{\partial T}{\partial y} + \rho D_{AB}\left(h_A \frac{\partial K_A}{\partial y} + h_B \frac{\partial K_B}{\partial y}\right)\right]_W - (\rho v)_W h_W[g] + (\rho v)_W h_W[l]. \tag{15}$$

This balance is also illustrated in figure 2. Using the heat of vaporization for water defined by $L_v = h_{BW} - h_W[l]$ and (14) with the condition $\lambda = 1$, we may write (15) in the form

$$\dot{q}_W[l] = k\frac{\partial T}{\partial y}\bigg|_W + \rho D_{AB}\frac{L_v}{K_{AW}}\frac{\partial K_B}{\partial y}\bigg|_W \tag{16}$$

Combination of (1), (11), (12) and (16) with the condition $\sigma = 0{\cdot}700$ then gives the stagnation melt rate for a hemisphere of ice in humid air,

$$w_i\sqrt{\frac{R}{U_0\nu}} = 1{\cdot}160\frac{\rho}{\rho_i}H, \tag{17}$$

where the dimensionless enthalpy transfer parameter H is defined by the equation

$$H = \frac{\overline{C_p}(T_0 - T_W)}{L_f} + \frac{L_v}{L_f}\left(\frac{K_{B0} - K_{BW}}{1 - K_{BW}}\right).$$

It should be emphasized that the numerical constant in (17) is valid only for $\sigma = 0{\cdot}700$. The only variable in the above result which needs further discussion is K_{BW}. The equilibrium value for K_{BW} would be the ratio of the density of saturated

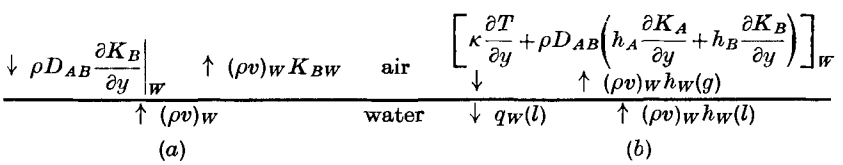

FIGURE 2. Mass and energy balances at the air–water interface.
(a) balance of water mass; (b) energy balance.

water vapour at the melt temperature (T_W) to the local density. A theoretical determination of the departure from the equilibrium value requires a detailed analysis of the evaporation and adsorption processes such as that given by Bauer & Zlotnick (1958). In the present work it is assumed that the equilibrium value is applicable.

The above solution has been obtained by neglecting the presence of the water layer. To check this assumption an approximate solution for the flow and heat transfer in the water layer will be found. First, however, the requirement that $f(0) \ll 1$ will be considered. From (6), (12) and (14) with $\sigma = 0{\cdot}700$, it is found that

$$f(0) = 0{\cdot}472\frac{K_{B0} - K_{BW}}{1 - K_{BW}}. \tag{18}$$

If the velocity at the air–water interface is small compared with the velocity at the outer edge of the air boundary layer then $f'(0) \ll 0$. To determine this quantity the water layer is assumed to have a thickness δ_l independent of x and a velocity distribution linear in both x and y, $u = Gxy$. The validity of these choices has been discussed in some detail by Roberts (1958). Conservation of mass in the water layer gives

$$\rho_l G\delta_l^2 = \rho_i w_i - (\rho v)_W. \tag{19}$$

The continuity of stress at the air–water interface requires that

$$G = 2{\cdot}41\frac{\mu}{\mu_l}\frac{U_0}{R}\left(\frac{U_0}{\nu R}\right)^{\frac{1}{2}} \tag{20}$$

In the present notation $u(0) = Gx\delta_l$, so combination of (6), (12), (14), (17), (19) and (20) gives, with the assumption $1+\frac{L_f}{Lv} \doteqdot 1$,

$$f'(0) = 1{\cdot}118\frac{\rho}{\rho_l}\left(\frac{\nu}{\nu_l}H\right)^{\frac{1}{2}} \tag{21}$$

A similar method may be used to determine whether the temperature at the outer edge of the water layer is significantly larger than the melt temperature. If $g_T = (T-T_W)/(T_0-T_W)$, the required inequality is $g_T(0) \ll 1$. Assuming a linear temperature profile $T = Ay+T_W$ we obtain

$$k_l A = \dot{q}_W[l] \tag{22}$$

for the continuity of heat flux at the air–water interface. Then using (12), (13), (16), (19), (20) and (22), we find that

$$g_T(0) = 0{\cdot}565\frac{k}{k_l}\sqrt{\left(\frac{\nu_l}{\nu}\right)}\frac{L_f}{\overline{C_p}(T_0-T_W)}H^{\frac{3}{2}}. \tag{23}$$

To estimate the heat convected away in the water layer a quadratic temperature distribution is assumed for the water layer, $T = Ay+By^2+T_W$. The continuity of heat flux at the air–water interface gives

$$k_l(A+2B\delta_l) = \dot{q}_W[l]. \tag{24}$$

The difference in energy flux between the air–water interface and the ice–water interface is equated to the heat convected away in the water boundary layer to obtain the second required equation,

$$\dot{q}_W[l]-k_lA-(\rho v)_W c_l(A\delta_l+B\delta_l^2) = c_l(\rho_i w_i-(\rho v)_W)\,(\tfrac{2}{3}A+\tfrac{1}{2}B\delta_l)\,\delta_l, \tag{25}$$

where c_l is the specific heat of water. If a shielding parameter S is defined by $S = \{k_lA-q_W[l]\}/\{q_W[l]\}$, the convective losses in the water layer may be neglected if $S \ll 1$. The shielding parameter may be evaluated from (12), (13), (16), (17), (19), (20), (24) and (25). Thus

$$S = 0{\cdot}538\sigma_l\frac{\rho}{\rho_l}\sqrt{\left(\frac{\nu}{\nu_l}\right)}H^{\frac{3}{2}}. \tag{26}$$

The validity of the assumptions will be checked when specific experimental conditions are considered.

3. Experiments

The stagnation point ablation of a hemispheric model fabricated from ice was determined in a subsonic wind tunnel. The experiments were carried out in the 40×36 in. closed circuit subsonic wind tunnel at the U.S. Naval Postgraduate School, Monterey, California. The humidity of the air in the tunnel was controlled by a fine water spray. This method provided a constant moisture content at any

level above the atmospheric value. The water vapour content was measured with an Aminco–Dunmore electric hygrometer.

The ice models were cast in hemispherical moulds. Models with nominal radii of 2 and 4 in. were used. To obtain reproducible results ice was required which did not contain air bubbles. To accomplish this the standard commercial technique was utilized. While the model was freezing, air was bubbled through the distilled water. The agitation produced ice which was optically clear in the region melted during the experiments. For some time before it was used each model was stored at a temperature just below 32 °F.

When models which contained air bubbles were ablated deep erosions occurred. It is hypothesized that the irregularities in the ice induced transition in the external boundary-layer flow; this in turn increased the local heat transfer and rate of melting, causing deep cavities. Using ice free of air bubbles, steady ablation was observed over the full range of free-stream velocities available. The model remained hemispherical.

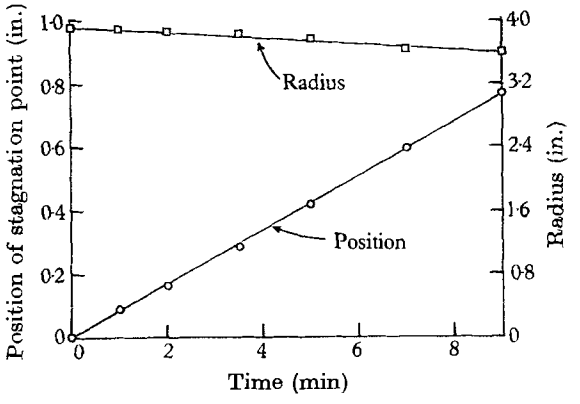

FIGURE 4. Dependence of the radius and stagnation point position on time; $U_0 = 237$ ft./sec, $T_0 = 84{\cdot}2$ °F, $\rho_{E0} = 1{\cdot}573 \times 10^{-3}$ lb./ft.^{3}, $w_i = 1{\cdot}066 \times 10^{-4}$ ft./sec.

Quantitative measurements of the rate of ablation at the stagnation point were obtained for fixed values of the free-stream velocity, temperature, and humidity. The range of free-stream velocities was from 40 to 250 ft./sec, the free-stream temperature was near 85 °F, the free-stream relative humidity ranged from 20 to 90%, and models with radii of 2 and 4 in. were used. During each run the model was photographed at regular intervals; a sequence of these photographs is shown in figure 3 (plate 1). The screen at the base of the hemisphere was used to control splashing during fabrication. From the photographs the position of the stagnation point was determined using an optical comparator. The radius of the hemisphere as a function of time was also determined from the photographs. These variables are plotted against time in figure 4 for the same run that is illustrated in figure 3. The constant slope of the position curve gives the rate of ablation at the stagnation point. From (17) this rate depends on the square root of the radius so that any change in slope should indeed be negligible.

For this representative run the validity of the approximations used in the analysis may be checked by using (18), (21), (23) and (26). The numerical values

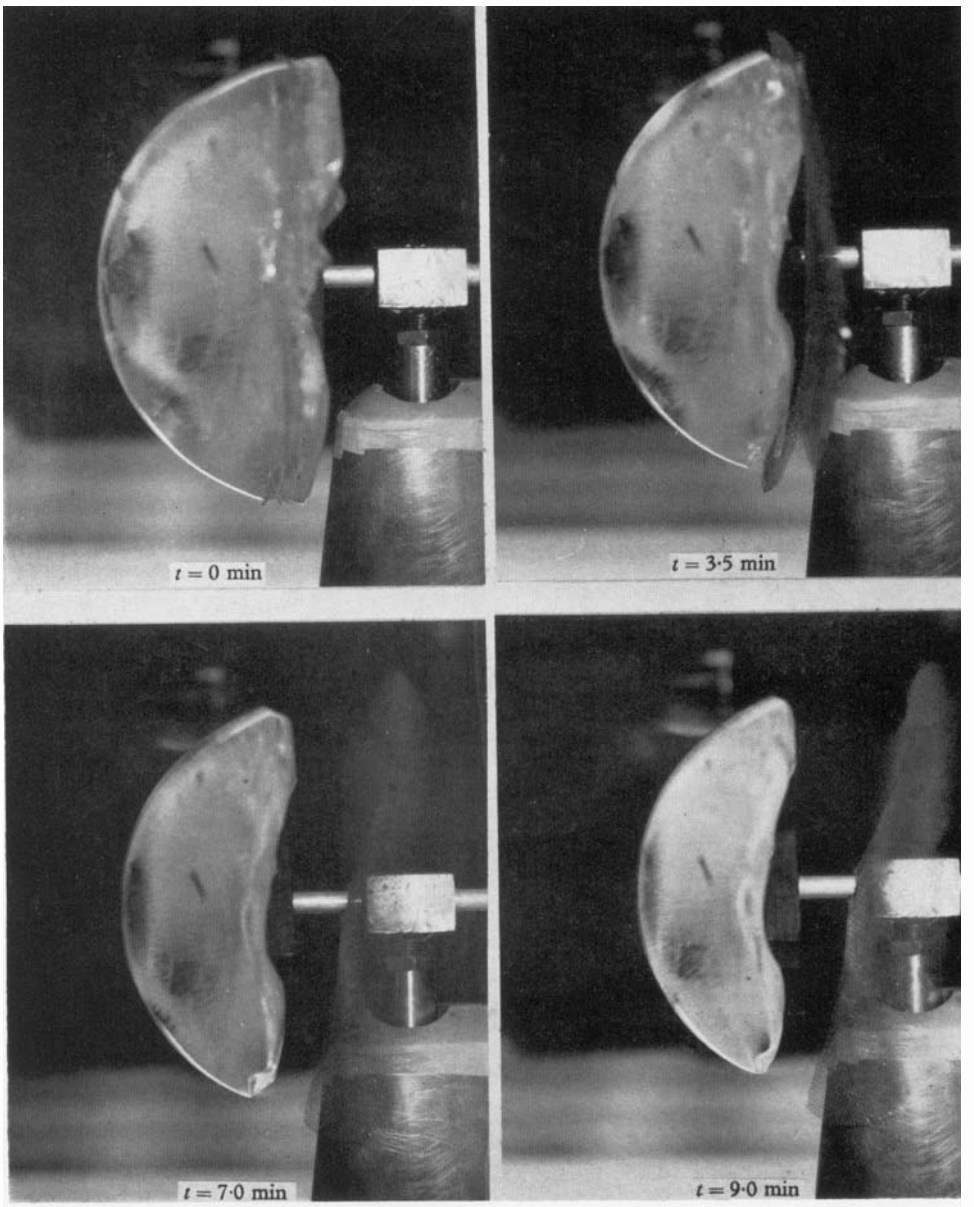

FIGURE 3 (plate 1). Photographs of an ablating hemisphere of ice; $U_0 = 237$ ft./sec., $T_0 = 84{\cdot}2$ °F, $\rho_{B0} = 1{\cdot}573 \times 10^{-3}$ lb./ft.^{3}.

obtained are $f(0) = 0{\cdot}845 \times 10^{-2}$, $f'(0) = 0{\cdot}182 \times 10^{-2}$, $g_T(0) = 1{\cdot}07 \times 10^{-2}$, and $S = 0{\cdot}135 \times 10^{-2}$. Since all values are considerably less than one the neglect of the water layer and the finite injection velocity at the air–water interface seems appropriate for the experimental conditions considered.

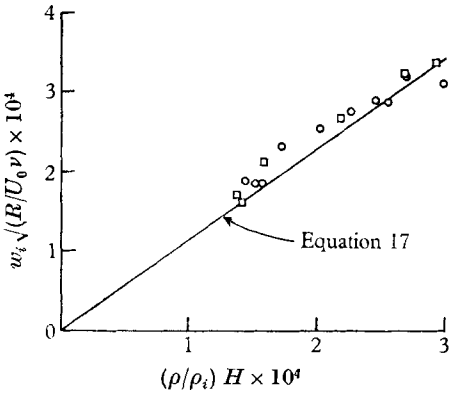

FIGURE 5. Dependence of the dimensionless melt rate on the enthalpy transfer parameter; $T_0 \doteq 85$ °F, $\rho_{B_0} = 0{\cdot}55 - 1{\cdot}60 \times 10^{-3}$ lb./ft., $U_0 = 40$–250 ft./sec. □, $R = 2$ in.; ○, $R = 4$ in.

All measurements are plotted in figure 5 in terms of the dimensionless variables obtained from the theory. Equation (17) is plotted for comparison. The variation in the enthalpy transfer parameter was obtained by varying the free-stream moisture content. The value of K_{BW} was obtained from the density of saturated water vapour at 32 °F ($\rho_{BW} = 0{\cdot}303 \times 10^{-3}$ lb./ft.^{3}). For all cases considered the density of water vapour in the free stream was higher than the wall value so that moisture actually condensed at the air–water interface. It is interesting to note that this condensation caused from 30 to 70% of the ablation. This rather surprising result is due to the large heat of vaporization for water. The agreement between theory and experiment seems adequate.

REFERENCES

BAUER, E. & ZLOTNICK, M. 1958 *Physics of Fluids*, **4**, 355.

LEES, L. 1958 *Combustion and Propulsion*, p. 451. 3rd AGARD Colloquium. London: Pergamon Press.

ROBERTS, LEONARD 1958 *J. Fluid Mech.* **4**, 505.

SCHLICHTING, H. 1955 *Boundary Layer Theory*. New York: McGraw-Hill.

SIBULKIN, M. 1952 *J. Aero. Sci.* **19**, 570.